DOI: 10.32615/ps.2019.167 PHOTOSYNTHETICA 58 (SI): 391-398, 2020

Special issue in honour of Prof. Reto J. Strasser

Effect of AtLFNR1 deficiency on chlorophyll *a* fluorescence rise kinetics OJIP of *Arabidopsis*

Y. GUO[*], Y. ZHANG[*], Y. LU[*], J. SHI[*], S. CHEN[*,+], R.J. STRASSER[*,**], S. QIANG[*], and Z. HU[***]

Weed Research Laboratory, Nanjing Agricultural University, 210095 Nanjing, China[*]
Bioenergetics Laboratory, University of Geneva, CH-1254 Jussy/Geneva, Switzerland[**]
Key Laboratory of Plant Stress Biology, School of Life Sciences, Henan University, 475004 Kaifeng, China[***]

Abstract

Leaf-type ferredoxin-NADP(H) oxidoreductase, encoded by *AtLFNR1* gene in *Arabidopsis*, extensively exists in chloroplast stroma and thylakoids and is responsible for the reduction of $NADP^+$ to NADPH in PSI. To investigate the relationship between the characteristics of chlorophyll *a* fluorescence transients OJIP and the function of AtLFNR1 protein, the fluorescence rise kinetics OJIP curves of *AtLFNR1* mutant leaves were determined. It is observed that *AtLFNR1* mutant has a lower level of variable fluorescence intensity relative to wild type, especially the J-step and the IP-phase. The JIP-test analysis suggests that the loss of AtLFNR1 function decreases clearly the oxidation rate of plastocyanin as well as PSI reaction center, damages slightly PSII antenna size and pigment assemblies, but stimulates distinctly the photosynthetic activity of PSII. Such multiple effects contribute to the change of shape characteristics of the OJIP transient curve in *AtLFNR1* mutant.

Additional key words: methyl viologen; MR_{820} signal; P_{700}.

Introduction

Photosynthesis is definitely the most important activity in plants. Ferredoxin-NADP(H) oxidoreductase (FNR) catalyzes the last step of photosynthetic electron transport in chloroplast, driving electrons from reduced ferredoxin (Fd) to $NADP^+$ (Rodriguez *et al.* 2007). In higher plants, a small nuclear multigene family encodes root and leaf FNR, which are two distinct forms of FNR (Morigasaki *et al.* 1993). The leaf FNR (LFNR) located in the stroma and thylakoids can generate a proton gradient across the thylakoid membrane to promote ATP production without accumulation of reducing equivalent (Johnson 2004). The change in pH generated by cyclic electron transfer is not only important for ATP production, but also for the induction of thermal dissipation of absorbed energy from PSII antennae. As key proteins linking light reactions and carbon assimilation, LFNRs take a part in response to environmental change *via* posttranslational modifications (Higuchi-Takeuchi *et al.* 2011, Lehtimäki *et al.* 2014). Moreover, LFNR involves in the import of proteins to chloroplast and is implicated in NDH-1 complex, cytochrome b_6/f as well as in PSI (Andersen *et al.* 1992). *AtLFNR1* encodes a kind of LFNR enzymes in *Arabidopsis thaliana*. There are two paralogous forms of LFNR in *A. thaliana*, AtLFNR1 and AtLFNR2, which are encoded by *At5g66190* and *At5g20020*, respectively (Hanke *et al.* 2005). AtLFNR1 was reported to help AtLFNR2 attach to thylakoid membrane. Their dimer formation might contribute to the electron distribution between linear and cyclic electron transfer pathways in different environment (Lintala *et al.* 2007). Compared to AtLFNR2, AtLFNR1 mainly located in the thylakoid fraction shows stronger affinity to ferredoxin isoforms (Kozuleva *et al.* 2016). Obviously, the AtLFNR1 plays a vital role in photosynthesis process of *A. thaliana*.

A rapid response of photosynthetic machine to stress is necessary for plants' survival in variable environment. Chlorophyll (Chl) *a* fluorescence shows an excellent dominance for measuring photosynthetic activity of plants

Received 5 September 2019, *accepted* 11 December 2019.
[+]Corresponding author; phone/fax: +86-25-84395117, e-mail: chenshg@njau.edu.cn
Abbreviations: ABS – absorption flux; Chl *a* – chlorophyll *a*; CS – excited leaf cross section; ET_0 – energy flux for electron transport; F_O, F_V, F_M – the initial, variable, and maximal fluorescence; Fd – ferredoxin; F_J – fluorescence at the J-step; FNR – ferredoxin- NADP(H) oxidoreductase; k_n – nonphotochemical quenching coefficient; k_p – photochemical quenching coefficient; MV – methyl viologen; OEC – oxygen-evolving complex; P_{700} – PSI reaction center; PC – plastocyanin; PQ – plastoquinone; Q_A – primary quinone electron acceptor of PSII; Q_B – secondary quinone electron acceptor of PSII; RC – reaction center; ROS – reactive species oxygen; t_{F_M} – time to reach maximal fluorescence F_M; TR_0 – trapping.
Acknowledgements: This work was supported by the National Key Research and Development Program (2017YFD0201300) and the Foreign Expert Project (G20190010118).

because of its noninvasive, precise, and quick characteristic. During recent three decades, the fast Chl *a* fluorescence rise kinetics OJIP has been extensively used to study plant physiology and plant stress. It has become a wonderful tool to monitor and quantify the behavior and performance of the photosynthetic apparatus, especially PSII (Strasser and Govindjee 1992, Strasser *et al*. 1995, 2004).

Generally, a typical fast Chl fluorescence rise OJIP curve shows a polyphasic transient from the initial (F_O) to the maximal fluorescence (F_M), being labeled step O (20 μs, all RCs open), J (~2 ms), I (~30 ms), and P (equal to F_M when all RCs are closed) (Strasser and Strasser 1995, Strasser *et al*. 2004). Numerous studies have suggested that the characteristics of the OJIP transient curve for a plant is different under different stress conditions. In fact, the OJIP curve performs changes in the case of suffering different stress or functional loss of related proteins (Strasser 1997, Strasser *et al*. 2004, 2010; Goltsev *et al.* 2012, Kalaji *et al.* 2012, 2014; Chen *et al*. 2016). The shape changes of the fluorescence O-J-I-P transient can be analyzed by the so-called 'JIP-test', which is based on 'Theory of Energy Fluxes in Biomembranes'. Recently, the JIP-test has been further developed to localize the effect on the PSII architecture and behavior (Strasser *et al*. 2004, 2010; Chen *et al.* 2014). However, some difficulties in this field still need to be overcome.

Here, our aim is to clarify the correlation between the change of characteristic shape of the fluorescence rise kinetics OJIP curve and the function of *AtLFNR1* gene. Based on the difference of the fast fluorescence rise kinetics OJIP of *Arabidopsis* leaves between wild type and *AtLFNR1* mutant, the absence of AtLFNR1 does indeed change the characteristics of the polyphasic rise OJIP curve due to the multiple effects on PSI and PSII.

Materials and methods

Plant materials and chemicals: *A. thaliana* wild type (Col-0) and T-DNA insertion mutant SALK-085403C (a homozygote line in SALK, *AtLFNR1*) obtained from *Arabidopsis* Biological Resource Center (ABSC, Ohio State University, USA) were utilized. The *AtLFNR1* mutant plant was identified by standard PCR protocols with primers specific to the 3' and 5' flanking sequence of target gene together with a T-DNA-specific primer before the experiment (not shown). The plants were grown in soil (nutrition-free peat moss:vermiculite = 1:3, v/v) in control environment chamber with 16 h light at PAR of 100 μmol(photon) m^{-2} s^{-1}, at 22°C, and 70% humidity. Three-week-old plants were used for further experiments.

Methyl viologen (MV, CAS No. 75365-73-0, 1,1'-dimethyl-4,4'-bipyridinium-dichloride) and methanol were obtained from *Sigma-Aldrich*. The stock solution of 100 mM MV was prepared in 100% methanol and diluted in distilled water as required for further experiments.

The expression level of *AtLFNR1* gene: Total RNA was isolated from mature leaves using *TRNzol Reagent* (*Tiangen*). *PrimeScript™ RT* reagent kit with gDNA Eraser (Perfect Real Time) from *TAKARA* was used for reverse transcription. Real-time PCR was performed according to the protocol of the *Mastercycler Realplex* (*Eppendorf*). PCR was performed using *SYBR Green Real-Time PCR Master Mix* (*TAKARA*), and the product was analyzed by the *Mastercycler ep Realplex* real-time quantitative (q)PCR system. The primer is used as the following: forward 5'-CACAAATGATGGCGGAGAGA-3', reverse 5'-CCAACAGGTCCAGTGATCTTAG-3'.

MV treatment: The detached, intact leaves of Col-0 were immerged for 10 min in 200 μM MV solution with 0.2% methanol. Before fluorescence measurement, the leaves were dark-adapted for 0.5 h in room temperature.

Chl *a* fluorescence rise kinetics measurement and JIP-test: The fluorescence rise kinetics OJIP curves of the detached intact leaves of Col-0 and *AtLFNR1* mutant were determined using a plant efficiency analyzer (*Handy PEA* fluorometer, *Hansatech Instruments Ltd.*, King's Lynn, Norfolk, UK). Before measurement, the samples were kept for 0.5 h in complete darkness at 25°C. A continued red light [650 nm, PAR of 3,500 μmol(photon) m^{-2} s^{-1}] was provided to induce the fluorescence transients OJIP curve. The experiment was repeated three times with at least 30 repetitions. The raw fluorescence data were transferred by *Handy PEA V1.30* software and analyzed by *BiolyzerHP3* software.

Each fluorescence rise kinetics curve was analyzed according to the JIP-test (Strasser *et al*. 2004). The following data from the original measurements were used: F_O (the fluorescence intensity at 20 μs), F_L (the fluorescence intensity at 150 μs), F_K (the fluorescence intensity at 300 μs), F_J (the fluorescence intensity at 2 ms), F_I (the fluorescence intensity at 30 ms), and the maximal fluorescence intensity F_M is equal to F_P. The JIP-test represents a translation of the raw experimental data to biophysical parameters (Strasser *et al*. 2004; Appendix) that quantify PSII behavior including conformation, structure, and function. The parameters which refer to time zero include: the maximum quantum yield of PSII primary photochemistry ($\varphi_{Po} = TR_0/ABS = F_V/F_M$), the efficiency that a trapped exciton moves an electron into the electron transport chain beyond the reduced Q_A form (Q_A^-) ($\psi_{E0} = ET_0/TR_0$), the quantum yield of electron transport ($\varphi_{Eo} = ET_0/ABS$), the average fraction of open RCs of PSII in the time span between 0 to t_{F_M} (S_m/t_{F_M}), the fraction of active PSII RCs per CS (RC/CS), absorption flux per CS (ABS/CS), trapped energy flux per CS (TR_0/CS), electron transport flux per CS (ET_0/CS), absorption flux per RC (ABS/RC), the quantum yield for the reduction of the end electron acceptors at the PSI acceptor side ($\varphi_{Ro} = RE_0/ABS$), and the probability that an electron is transported from the reduced intersystem electron acceptors to final electron acceptors of PSI ($\delta_{Ro} = RE_0/ET_0$).

The performance index for energy conservation from photons absorbed by PSII to the reduction of intersystem electron acceptors (PI_{ABS}), and the performance index for energy conservation from photons absorbed by PSII to the

reduction of PSI end acceptors (PI_{total}) were introduced (Strasser *et al.* 2004, 2010):

$$PI_{ABS} = \frac{\gamma_{RC}}{1-\gamma_{RC}} \times \frac{\varphi_{Po}}{1-\varphi_{Po}} \times \frac{\psi_{Eo}}{1-\psi_{Eo}}$$

$$PI_{total} = PI_{ABS} \times \delta_{Ro}/(1-\delta_{Ro})$$

where γ_{RC} is the fraction of reaction center chlorophyll (Chl_{RC}) per total chlorophyll ($Chl_{RC} + Chl_{Antenna}$), therefore $\gamma_{RC}/(1-\gamma_{RC}) = Chl_{RC}/Chl_{Antenna} = RC/ABS$.

The modulated 820 nm reflection (MR_{820}): The MR_{820} signal measurements of Col-0 and *AtLFNR1* mutant were performed by a *Multifunctional-PEA* fluorometer (*Hansatech Instruments Ltd.*, King's Lynn, UK). The MR signal at 820 nm was measured at the modulated light from LED (820 ± 25 nm, 50% of the maximal intensity). Measurements were conducted for an induction period of 10 s. The experiment was performed with at least 20 repetitions. The raw data of the MR_{820} signals were analyzed by the in-house software *M-PEA data Analyzer v. 5.3*. The ratio MR/MR_0 was calculated, where MR_0 is the value at the onset of the actinic illumination (taken at 0.7 ms, the first reliable MR measurement). An increase of the fraction MR/MR_0 indicates a decrease in the concentration of the oxidized states of plastocyanin (PC^+) and PSI RC (P_{700}^+), which is due to PC^+ and P_{700}^+ reduction (Strasser *et al.* 2010).

Statistical analysis: One-way analysis of variance (*ANOVA*) was carried out and means were separated by *Duncan*'s LSD at 95% using *SPSS Statistics 20.0*.

Results

Fluorescence rise kinetics O-J-I-P curves: The *AtLFNR1* knockout mutant shows a smaller rosette size and light green leaves compared with Col-0 (Fig. 1). Such phenotype suggests that AtLFNR1 deficiency affects the photosynthesis process. Consequently, it is expected that the difference should exist in the fluorescence rise kinetics OJIP curve of Col-0 and *AtLFNR1* mutant leaves. In Fig. 2*A*, the fluorescence transient curves of Col-0 and *AtLFNR1* mutant were presented. In addition, MV, a classical PSI herbicide inhibiting electron transfer from FeS cluster to FNR, was also used to treat Col-0 leaves as the positive control. Clearly, the fluorescence induction transient curves of Col-0 and *AtLFNR1* mutant as well as MV-treated Col-0 leaves exhibited a typical polyphasic O-J-I-P shape. However, there were several differences in the details. Comparing the dark-adaptation kinetics of Col-0 leaves, a decrease of the variable fluorescence intensity (F_t) from F_O to F_M in *AtLFNR1* mutant was observed. For MV-treated Col-0 leaves, the IP-phase was suppressed, but the fluorescence kinetics curve up to 30 ms (I-step) was not affected.

To further analyze the effect of AtLFNR1 deficiency on the kinetics OJIP properties, the fluorescence curves double normalized by F_O (20 μs) and F_M were presented

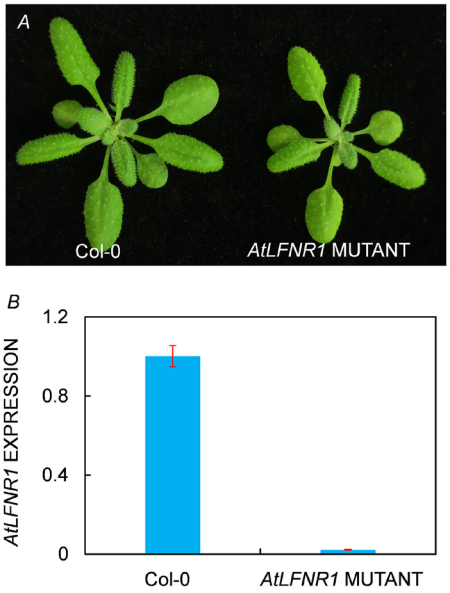

Fig. 1. (*A*) Phenotypes of *Arabidopsis* wild type (Col-0) and *AtLFNR1* mutant and (*B*) their expression level of *ATLFNR1* gene. Mutant plant significantly decreases rosette size and biomass with nearly no *ATLFNR1* gene expression compared to Col-0.

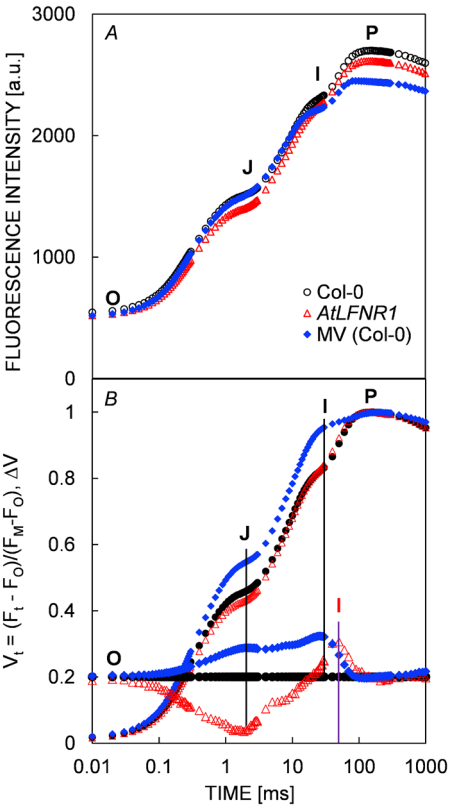

Fig. 2. Chl *a* fluorescence rise kinetics of *Arabidopsis* Col-0, *AtLFNR1* mutant, and MV-treated Col-0. (*A*) Raw fluorescence rise kinetics. (*B*) Fluorescence rise kinetics normalized by F_O and F_M as $V_t = (F_t - F_O)/(F_M - F_O)$ (*top*), and $\Delta V_t = Vt_{(AtLFNR1 \text{ or MV-treated Col-0})} - V_{t(Col-0)}$ (*bottom*). Each curve is the average of 30 measurements.

as relative variable fluorescence $V_t = (F_t - F_O)/(F_M - F_O)$ (*top*) and ΔV_t (*bottom*) *vs*. logarithmic time scale (Fig. 2*B*). Compared with Col-0, the fluorescence curve of *AtLFNR1* mutant showed a remarkable lowering in the J-step level and a considerable increase in the I-step level. Moreover, the JI-phase was prolonged; the time to reach I-step was at 50 ms not 30 ms. In the case of MV, we observed a significant increase of the level of J-step and I-step due to a strong decrease in the IP-phase.

In Fig. 3, to confirm the events reflected in the OK, OJ, OI, and IP-phase, other normalizations and corresponding subtractions (difference kinetics) of the fluorescence kinetics curves were also presented. As shown in Fig. 3*A*, the fluorescence rise kinetics curves of Col-0, *AtLFNR1* mutant and MV-treated Col-0 leaves were double normalized by 50 μs and K-step (300 μs), as $W_{OK} = (F_t - F_O)/(F_K - F_O)$ kinetics (*top*), and plotted with the difference kinetics $\Delta W_{OK} = W_{OK(AtLFNR1 \text{ or MV-treated Col-0})} - W_{OK(Col-0)}$ (*bottom*) in the linear time scale from 50–300 μs. This results in appearance of the L-band hidden between the steps O and K. The L-band is an indicator of the energetic connectivity or grouping of the PSII units (Strasser *et al*. 2004). The W_{OK} curves of *AtLFNR1* mutant and MV-treated Col-0 coincide well with that of Col-0, and ΔW_{OK} curves of these three in a straight line. It is indicated that AtLFNR1 deficiency does not affect the OK-phase and the L-band. The similar results were also found in the W_{OJ} (*top*) and ΔW_{OJ} curves (*bottom*). Furthermore, a visible K-step was not elicited in *AtLFNR1* mutant and MV-treated Col-0 (Fig. 3*B*). In Fig. 3*C*, the fluorescence kinetics curves were normalized between F_O and F_I (30 ms), as $W_{OI} = (F_t - F_O)/(F_I - F_O)$ (*top*), and difference kinetics $\Delta W_{OI} = W_{OI(AtLFNR1 \text{ or MV-treated Col-0})} - W_{OI(Col-0)}$ (*bottom*) on logarithmic time scale. The biggest change was a significant decrease in J-step of *AtLFNR1* mutant relative to Col-0. Additionally, the IP-phase of *AtLFNR1* mutant was slightly lower than that of Col-0. The major change of MV-treated Col-0 was a distinct decrease of the IP-phase, but MV did not influence on the part from O-step *via* J-step to I-step of kinetics curve. According to the W_{OI} (only ≥ 1 is shown) plotted in the linear 30–530-ms time range, the IP-phase of *AtLFNR1* mutant decreased mildly, and the IP-phase of MV-treated Col-0 decreased sharply (Fig. 3*D*).

The JIP-test analysis: In order to further assess the effect of AtLFNR1 deficiency on the photosynthesis, several JIP-test parameters, quantifying the conformation, structure, and function of photosynthetic apparatus, were provided in Fig. 4. For *AtLFNR1* mutant, a little decrease in F_O, F_M, F_J, and F_I was observed compared with that of Col-0. Among these four parameters, the value of F_J of *AtLFNR1* mutant was reduced by 7% (Fig. 4; Table 1S, *supplement*). It indicated that the Q_A^- was accumulating at a slower rate in *AtLFNR1* mutant. An increase more than 5% in φ_{Eo}, ψ_{E0}, and k_p means that AtLFNR1 deficiency accelerated PSII electron transfer rate and increased the capacity of photochemical reaction (Fig. 4, Table 1S). This is possible the reason that the accumulation of Q_A^- was slowed down, showing a decrease in the F_J level. In addition, the parameters including S_m/t_{F_M}, RC/CS_0, ABS/CS_0, TR_0/CS_0, φ_{Ro}, and δ_{Ro} showed a decrease of about 5% in *AtLFNR1* mutant. The value of φ_{Po}, ET_0/CS_0, ABS/RC, γ_{RC}, k_n, and PI_{total} remained nearly unchanged relative to Col-0 (Fig. 4, Table 1S). Such results demonstrate that there is somewhat negative effect of AtLFNR1 deficiency on the amount of PSII active RCs, Chl concentration, as well as architecture

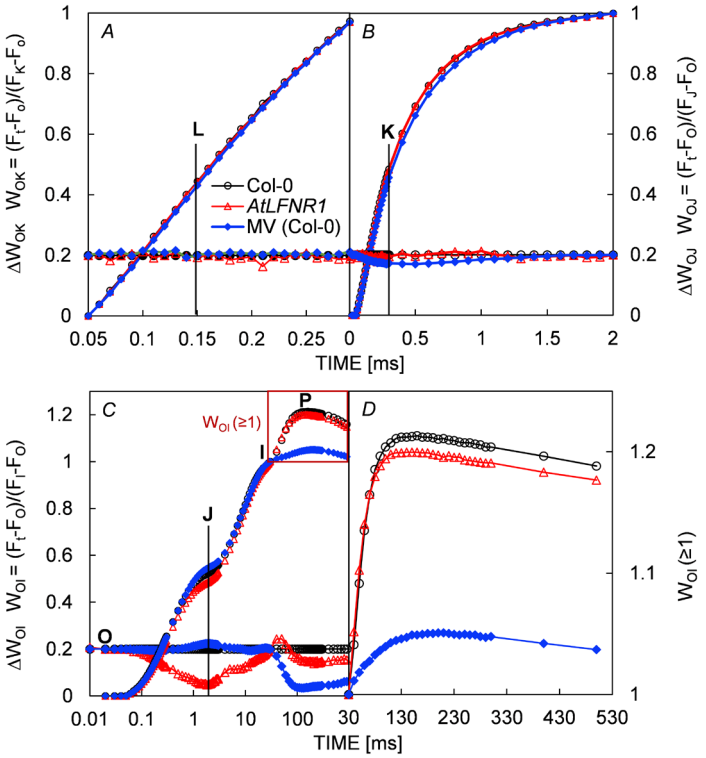

Fig. 3. Different normalizations of the fluorescence rise kinetics curves of *Arabidopsis* Col-0, *AtLFNR1* mutant, and MV-treated Col-0. (*A*) Fluorescence rise kinetics normalized by F_O and F_K as $W_{OK} = (F_t - F_O)/(F_K - F_O)$ (*top*), and the difference kinetics $\Delta W_{OK} = W_{OK(AtLFNR1 \text{ or MV-treated Col-0})} - W_{OK(Col-0)}$ (*bottom*). (*B*) Fluorescence rise kinetics normalized by F_O and F_J as $W_{OJ} = (F_t - F_O)/(F_J - F_O)$ (*top*), and the difference kinetics $\Delta W_{OJ} = W_{OJ(AtLFNR1 \text{ or MV-treated Col-0})} - W_{OJ(Col-0)}$ (*bottom*). (*C*) Fluorescence rise kinetics normalized by F_O and F_I as $W_{OI} = (F_t - F_O)/(F_I - F_O)$ (*top*) and the difference kinetics $\Delta W_{OJ} = W_{OJ(AtLFNR1 \text{ or MV-treated Col-0})} - W_{OJ(Col-0)}$ (*bottom*). (*D*) Fluorescence rise kinetics of $W_{OI} \geq 1$ on a linear time scale from 30 ms to 530 ms to show the IP-phase. Each curve is the average of 30 measurements.

of PSII pigment assemblies, and the reduction of the end electron acceptors at the PSI acceptor side. However, absence of AtLFNR1 does not change significantly the maximum quantum yield of primary photochemistry and the average antenna size per RC. It is notable that the performance index PI_{ABS} of *AtLFNR1* mutant was 15% of that in Col-0 (Fig. 4, Table 1S). Obviously, AtLFNR1 deficiency stimulates PSII energy conservation efficiency, exhibiting a clear rise in PSII overall photosynthetic activity.

For MV-treated Col-0 leaves, MV did not affect significantly F_J, φ_{Po}, k_p, ABS/RC, and γ_{RC}, but decreased the value of F_O, F_I, and F_M declined by 5, 4, and 9%, relative to control, respectively (Fig. 4, Table 1S). ABS/CS_0 and TR_0/CS_0 showed an around decrease of 9 and 11%. The ET parameters φ_{Eo}, ψ_{Eo}, and ET_0/CS_0 declined by 14, 13, and 22% compared with control. It is clear that MV can reduce

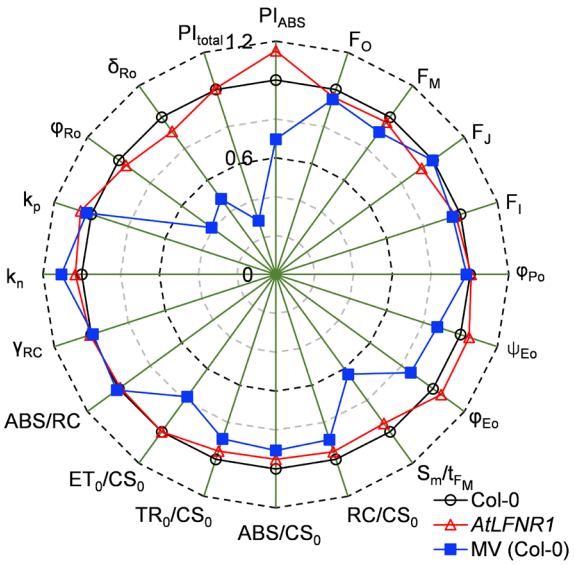

Fig. 4. Spider plot presentation of several JIP-test parameters quantifying PSII structure and function of the photosynthetic apparatus of *Arabidopsis* Col-0, *AtLFNR1* mutant, and MV-treated Col-0. Each parameter is expressed as fraction relatively to the values of Col-0 as the control.

PSII electron transfer efficiency, which leads to a decrease in the amount of PSII active RCs. In fact, RC/CS_0 and S_m/t_{F_M} decreased by 11 and 37%, respectively, after MV treatment. However, k_p in MV-treated leaves of Col-0 was about 10% higher than that of control. This suggests that a lot of energy dissipated as heat for the activation of PSII RCs in the presence of MV. It was observed that MV leads to a significant decrease in PSII overall photosynthetic activity since PI_{ABS} lowered by 30% in MV-treated leaves. In all parameters, the most affected were φ_{R0}, δ_{R0}, and PI_{total}, which decreased by 59, 52, and 71%, respectively (Fig. 4, Table 1S). It was proved that the greatest influence of MV was the strong inhibition of reduction of the end acceptors at the PSI electron acceptor side.

MR_{820} signal: To further prove the effect of AtLFNR1 deficiency on PSI, the MR_{820} signal of Col-0, *AtLFNR1* mutant, and MV-treated Col-0 were determined. Generally, there are two phases in the MR kinetics curve: a fast decrease phase from MR_0 (at around 0.7 ms) to MR_{min} (at around 10 ms) and a slow increase phase from MR_{min} to MR_{max} (at around 100 ms). The fast phase is related to the accumulation of PC^+ and P_{700}^+ and the slow one represents re-reduction of PC^+ and P_{700}^+ utilizing electrons from PSII. At MR_{min} of the MR/MR_0 kinetics, the oxidation and reduction rate achieve a balance point in the noncyclic electron flow. As shown in Fig. 5*A*, it is evident that the MR_{min} of *AtLFNR1* mutant was higher, but that of MV-treated Col-0 was much lower than that of Col-0. There was nearly no difference in the fast phase of the MR/MR_0 curves between Col-0 and MV-treated Col-0 leaves. This indicates that MV does not affect the capability of P_{700} to get oxidized. The MR/MR_0 kinetics of MV-treated Col-0 remained the steady same level after the MR_{min}. It is because MV captures electrons from PSI ahead of FNR at almost the same rate as PSII is pumping them to PSI (Schansker *et al.* 2005). The disappearance of the slow MR/MR_0 phase demonstrates that MV supports high rate of linear electron transport through PSI preventing PQ pool (and consequently P_{700}^+ and PC^+) full reduction after reaching equilibrium at MR_{min}. For *AtLFNR1* mutant, somewhat decrease in the amplitude of the fast and slow

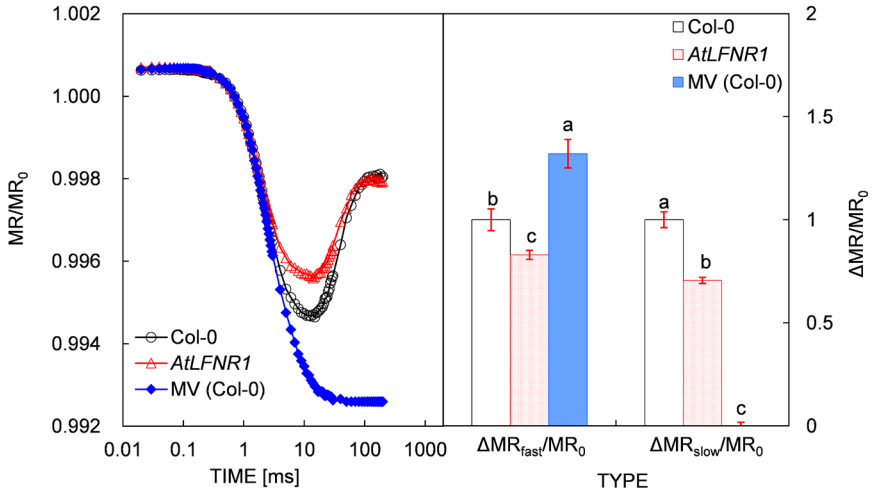

Fig. 5. (*A*) The modulated 820-nm reflection kinetics curves of *Arabidopsis* Col-0, *AtLFNR1* mutant, and MV-treated Col-0. The plotted values are expresses by the MR/MR_0 ratio. (*B*) The characteristic parameters of the MR/MR_0 kinetics curves of *Arabidopsis* Col-0, *AtLFNR1* mutant, and MV-treated Col-0. The amplitudes of the fast phase, $\Delta MR_{fast}/MR_0 = (MR_0 - MR_{min})/MR_0$ and of the slow phase, $\Delta MR_{slow}/MR_0 = (MR_{max} - MR_{min})/MR_0$.

MR/MR_0 phase was observed (Fig. 5*A*). It means that AtLFNR1 deficiency reduced slightly the capability of P_{700} to get oxidized, however, accelerated the re-reduction of P_{700}^+. In Fig. 5*B*, the characteristic parameters of MR/MR_0 kinetics, $\Delta MR_{fast}/MR_0$, and $\Delta MR_{slow}/MR_0$ were also calculated. The value of $\Delta MR_{fast}/MR_0$ and $\Delta MR_{slow}/MR_0$ of *AtLFNR1* mutant was about 83 and 71% of Col-0, respectively. The $\Delta MR_{fast}/MR_0$ of MV-treated Col-0 increased 32% relative to control. Obviously, unlike MV, AtLFNR1 deficiency really affected slightly the reduction rate and the oxidation rate of PSI.

Discussion

Arabidopsis AtLFNR1 mutant exhibited a smaller rosette size and less green leaves relative to wild type (Fig. 1), which is consistent well with previous study. Lintala *et al.* (2007) found that absence of AtLFNR1 decreased the rosette size, Chl content, light-harvesting complex proteins, FNR, as well as the electron pool in the intersystem chain, and CO_2 fixation, but the maximal quantum yield of PSII (F_V/F_M) kept nearly stable. Based on evidence from fast fluorescence rise kinetics, AtLFNR1 deficiency does not influence on L-band in the W_{OK} and K-band in W_{OJ} kinetics curve. Generally, the L-band is an indicator of the energetic connectivity or grouping of the PSII units, the K-band appearance is a signal of the inactivation of the oxygen-evolving complex (OEC) (Strasser *et al*. 2004). However, the performance index PI_{ABS}, expressing PSII overall photosynthetic activity, increased significantly by 15% in *AtLFNR1* mutant (Fig. 4, Table 1S). PI_{ABS} is produced by the three independent components φ_{Po}, ψ_{Eo}, and γ_{RC}. The maximum quantum yield of PSII primary photochemistry (φ_{Po}) and fraction of RC Chl in relation to total Chl (γ_{RC}) remained nearly unchanged in *AtLFNR1* mutant and wild type (Fig. 4; Strasser *et al*. 2004). The *AtLFNR1* mutant shows about 5% increase in the probability that an electron moves further than Q_A^- (ψ_{Eo}) and the quantum yield of PSII electron transport (φ_{Eo}) (Fig. 4, Table 1S). This is further supported by a visible decrease in the J-step level of *AtLFNR1* mutant (Figs. 3*C*, 4; Table 1S). It is well known that a quick rise of the J-step level attributes to the large accumulation of Q_A^- in PSII RCs, which is because of blocking electron flow from Q_A to Q_B (Strasser and Govindjee 1992, Strasser *et al*. 2004). In contrast, a lower level of the J-step might mean a higher electron transport rate at the acceptor side of PSII. Such results indicate that AtLFNR1 deficiency stimulates PSII overall photosynthetic activity, which is partly due to a slight increase of the efficiency of PSII electron transfer further than Q_A^-. Contrary to *AtLFNR1* mutant, MV somewhat decreases PSII electron transfer activity, the amount of the active PSII RCs, and the overall photosynthetic activity (Fig. 4, Table 1*S*). MV is a highly effective electron acceptor that competes strongly with Fd for electrons from the FeS clusters of PSI (Schansker *et al*. 2005).

As a PSI inhibitor, MV causes an extremely significant decrease in the IP-phase (Fig. 3*C*,*D*), φ_{Ro}, δ_{Ro}, and PI_{total} (Fig. 4, Table 1S). The IP-phase reflects the reduction of PSI electron acceptor, *i.e*., Fd, other intermediates, and NADP. For each W_{OI} curve, the maximal amplitude of the IP-phase kinetics curve indicates the size of the pool of the end electron acceptors at PSI acceptor side (Strasser *et al*. 2004, Yusuf *et al*. 2010). The IP-phase kinetics is also associated with the inactive FNR at the acceptor side of PSI (Schansker *et al*. 2005). Like MV, AtLFNR1 deficiency declined clearly the amplitude of the IP-phase kinetics curve and the value of φ_{Ro} and δ_{Ro}, but the effect was much weaker than that of MV treatment (Figs. 3*C*,*D*, 4; Table 1S). We demonstrated that *AtLFNR1* mutant has a slight negative effect on the reduction of the end electron acceptors at the PSI acceptor side. This was further proved by the data from the MR_{820} signal (Fig. 5). MV speeds up the oxidation rate of PC and P_{700} because it gets electrons faster than Fd, however, eliminates the re-reduction of PC^+ and P_{700}^+. Compared to wild type, *AtLFNR1* mutant revealed a lower oxidation rate of PC and P_{700} for the inactive FNR. Inhibition of FNR activity blocks electron transport from the reduced Fd to $NADP^+$ and produces ROS, which readily cause lipid peroxidation and Chl breakdown (Halliwell 1991). In fact, a mild decrease of ABS/CS_0 and TR_0/CS_0 in *AtLFNR1* mutant suggests that AtLFNR1 deficiency certainly reduces the Chl concentration and damages the architecture of PSII pigment assemblies (Fig. 4, Table 1S). According to the JIP-test, ABS/CS expresses the total absorption flux per CS, and can be taken as a measurement for the Chl concentration per CS or an average antenna size of PSII (Srivastava *et al*. 1998, Strasser *et al*. 2004). TR_0/CS refers to the trapped energy flux per CS, reflecting the efficiency of light energy transfer between antenna pigment molecules and from those to the PSII RCs (Strasser *et al*. 2004). A decrease in Chl antenna may also explain why *AtLFNR1* mutant has a slightly lower level of the variable fluorescence intensity (F_t) (Fig. 2*A*). The result is in good agreement with the fact that *AtLFNR1* gene knockout decreased the Chl content and light-harvesting complex proteins (Lintala *et al.* 2007).

In conclusion, Chl *a* fluorescence rise kinetics of *Arabidopsis* leaves is related to *AtLFNR1* gene. The loss of the FNR function in *AtLFNR1* mutant leads to multiple effects on two photosystems, showing a visible decrease in the oxidation rate of PC and P_{700}, a slight damage to the chlorophyll antenna and pigment assemblies of PSII, and a clear increase of PSII overall photosynthetic activity. As a result, the fluorescence rise kinetics OJIP of *AtLFNR1* mutant reveals a lower level of variable fluorescence intensity as well as the J-step, and a smaller amplitude of the IP-phase.

References

Andersen B., Scheller H.V., Møller B.L.: The PSI-E subunit of photosystem I binds ferredoxin:$NADP^+$ oxidoreductase. – FEBS Lett. **311**: 169-173, 1992.

Chen S., Strasser R.J., Qiang S.: *In vivo* assessment of effect of phytotoxin tenuazonic acid on PSII reaction centers. – Plant Physiol. Bioch. **84**: 10-21, 2014.

Chen S., Yang J., Zhang M. *et al*: Classification and characteristics of heat tolerance in *Ageratina adenophora* populations using fast chlorophyll *a* fluorescence rise O-J-I-P. – Environ. Exp.

Bot. **122**: 126-140, 2016.
Goltsev V., Zaharieva I., Chernev P. *et al.*: Drought-induced modifications of photosynthetic electron transport in intact leaves: Analysis and use of neural networks as a tool for a rapid non-invasive estimation. – BBA-Bioenergetics **1817**: 1490-1498, 2012.
Halliwell B.: Oxygen radicals: their formation in plant tissues and their role in herbicide damage. – In: Baker N.R., Percival M.P. (ed.): Herbicides. Pp. 87-129. Elsevier Science, Amsterdam-London-New York-Tokyo 1991.
Hanke G.T., Okutani S., Satomi Y. *et al.*: Multiple iso-proteins of FNR in *Arabidopsis*: Evidence for different contributions to chloroplast function and nitrogen assimilation. – Plant Cell Environ. **28**: 1146-1157, 2005.
Higuchi-Takeuchi M., Ichikawa T., Kondou Y. *et al.*: Functional analysis of two isoforms of leaf-type ferredoxin-$NADP^+$-oxidoreductase in rice using the heterologous expression system of *Arabidopsis*. – Plant Physiol. **157**: 96-108, 2011.
Johnson G.N.: Cyclic electron transport in C_3 plants: fact or artefact? – J. Exp. Bot. **56**: 407-416, 2004.
Kalaji H.M., Carpentier R., Allakhverdiev S.I., Bosa K.: Fluorescence parameters as early indicators of light stress in barley. – J. Photoch. Photobio. B **112**: 1-6, 2012.
Kalaji H.M., Oukarroum A., Alexandrov V. *et al.*: Identification of nutrient deficiency in maize and tomato plants by *in vivo* chlorophyll *a* fluorescence measurements. – Plant Physiol. Bioch. **81**: 16-25, 2014.
Kozuleva M., Goss T., Twachtmann M. *et al.*: Ferredoxin: NADP(H) oxidoreductase abundance and location influences redox poise and stress tolerance. – Plant Physiol. **172**: 1480-1493, 2016.
Krüger G.H.J., Tsimilli-Michael M., Strasser R.J.: Light stress provokes plastic and elastic modifications in structure and function of photosystem II in camellia leaves. – Physiol. Plantarum **101**: 265-277, 1997.
Lehtimäki N., Koskela M.M., Dahlström K.M. *et al.*: Posttranslational modifications of Ferredoxin-$NADP^+$ oxidoreductase in *Arabidopsis* chloroplasts. – Plant Physiol. **166**: 1764-1776, 2014.
Lintala M., Allahverdiyeva Y., Kidron H. *et al.*: Structural and functional characterization of ferredoxin-$NADP^+$-oxidoreductase using knock-out mutants of *Arabidopsis*. – Plant J. **49**: 1041-1052, 2007.
Morigasaki S., Jin T., Wada J.K.: Comparative studies on ferredoxin-$NADP^+$ oxidoreductase isoenzymes derived from different organs by antibodies specific for the radish root- and leaf-enzymes. – Plant Physiol. **103**: 435-440, 1993.
Rodriguez R.E., Lodeyro A., Poli H.O. *et al.*: Transgenic tobacco plants overexpressing chloroplastic ferredoxin-NADP(H) reductase display normal rates of photosynthesis and increased tolerance to oxidative stress. – Plant Physiol. **143**: 639-649, 2007.
Schansker G., Tóth S.Z., Strasser R.J.: Methylviologen and dibromothymoquinone treatments of pea leaves reveal the role of photosystem I in the Chl *a* fluorescence rise OJIP. – BBA-Bioenergetics **1706**: 250-261, 2005.
Srivastava A., Jüttner F., Strasser R.J.: Action of the allelochemical, fischerellin A, on photosystem II. – BBA-Bioenergetics **1364**: 326-336, 1998.
Strasser B.J.: Donor side capacity of photosystem II probed by chlorophyll *a* fluorescence transients. – Photosynth. Res. **52**: 147-155, 1997.
Strasser B.J., Strasser R.J.: Measuring fast fluorescence transients to address environmental questions: the JIP-test. – In: Mathis P. (ed.): Photosynthesis: From Light to Biosphere. Pp. 977-980. Kluwer Academic Publishers Press, Dordrecht 1995.
Strasser R.J., Govindjee: The Fo and the O-J-I-P fluorescence rise in higher plants and algae. – In: Argyroudi-Akoyunoglou J.H. (ed.): Regulation of Chloroplast Biogenesis. Pp. 423-426. Plenum Press, New York 1992.
Strasser R.J., Srivastava A., Govindjee: Polyphasic chlorophyll *a* fluorescence transient in plants and cyanobacteria. – Photochem. Photobiol. **61**: 32-42, 1995.
Strasser R.J., Tsimilli-Michael M., Qiang S., Goltsev V.: Simultaneous *in vivo* recording of prompt and delayed fluorescence and 820-nm reflection changes during drying and after rehydration of the resurrection plant *Haberlea rhodopensis*. – BBA-Bioenergetics **1797**: 1313-1326, 2010.
Strasser R.J., Tsimilli-Michael M., Srivastava A.: Analysis of the chlorophyll *a* fluorescence transient. – In: Papageorgiou G.C., Govindjee (ed.): Chlorophyll *a* Fluorescence: A Signature of Photosynthesis. Advances in Photosynthesis and Respiration. Pp. 321-362. Springer, Dordrecht 2004.
Yusuf M.A., Kumar D., Rajwanshi R. *et al.*: Overexpression of γ-tocopherol methyl transferase gene in transgenic *Brassica juncea* plants alleviates abiotic stress: physiological and chlorophyll *a* fluorescence measurements. – BBA-Bioenergetics **1797**: 1428-1438, 2010.

Appendix. Formulae and explanation of the technical data of the OJIP curves and the selected JIP-test parameters used in this study (Krüger *et al*. 1997, Strasser *et al*. 2004, 2010). Subscript '0' (or 'o' when written after another subscript) indicates that the parameter refers to the onset of illumination, when all RCs are assumed to be open.

Technical fluorescence parameters	
F_t	fluorescence at time t after onset of actinic illumination
$F_O \cong F_{20\mu s}$	minimal fluorescence, when all PSII RCs are open
$F_L \equiv F_{150\mu s}$	fluorescence intensity at the L-step (150 μs) of OJIP
$F_K \equiv F_{300\mu s}$	fluorescence intensity at the K-step (300 μs) of OJIP
$F_J \equiv F_{2ms}$	fluorescence intensity at the J-step (2 ms) of OJIP
$F_I \equiv F_{30ms}$	fluorescence intensity at the I-step (30 ms) of OJIP
F_P (= F_M)	maximal recorded fluorescence intensity, at the peak P of OJIP
$F_v \equiv F_t - F_O$	variable fluorescence at time t
$F_V \equiv F_M - F_O$	maximal variable fluorescence
t_{F_M}	time (in ms) to reach the maximal fluorescence intensity F_M

$V_t \equiv (F_t - F_O)/(F_M - F_O)$	relative variable fluorescence at time t
$V_J = (F_J - F_O)/(F_M - F_O)$	relative variable fluorescence at the J-step
$W_t \equiv (F_t - F_O)/(F_J - F_O)$	relative variable fluorescence F_v to the amplitude $F_J - F_O$
$W_{OK} = (F_t - F_O)/(F_K - F_O)$	ratio of variable fluorescence $F_t - F_O$ to the amplitude $F_K - F_O$
$W_{OJ} = (F_t - F_O)/(F_J - F_O)$	ratio of variable fluorescence $F_t - F_O$ to the amplitude $F_J - F_O$
$W_{OI} = (F_t - F_O)/(F_I - F_O)$	ratio of variable fluorescence $F_t - F_O$ to the amplitude $F_I - F_O$
Deexcitation rate constant of PSII antenna	
k_F	rate constant for fluorescence emission
$k_n = (ABS/CS) \times k_F \times (1/F_M)$	nonphotochemical deexcitation rate constant
$k_p = (ABS/CS) \times k_F \times (1/F_O - 1/F_M)$	photochemical deexcitation rate constant
Quantum efficiencies or flux ratios	
$\varphi_{Po} = PHI(P_0) = TR_0/ABS = 1 - F_O/F_M$	maximum quantum yield for primary photochemistry
$\psi_{Eo} = PSI_0 = ET_0/TR_0 = (1 - V_J)$	probability that an electron moves further than Q_A^-
$\varphi_{Eo} = PHI(E_0) = ET_0/ABS = (1 - F_O/F_M)\,(1 - V_J)$	quantum yield for electron transport (ET)
$\varphi_{Ro} = RE_0/ABS = \varphi_{Po} \times \varphi_{Eo} \times \delta_{Ro} = \varphi_{Po} \times (1 - V_I)$	quantum yield for reduction of the end electron acceptors at the PSI acceptor side (RE)
$\delta_{Ro} = RE_0/ET_0 = (1 - V_I)/(1 - V_J)$	probability that an electron is transported from the reduced intersystem electron acceptors to the final electron acceptors of PSI (RE)
$\gamma_{RC} = Chl_{RC}/Chl_{total} = RC/(ABS+RC)$	probability that a PSII Chl molecule functions as RC
Phenomenological energy fluxes (per excited leaf cross-section, CS)	
$ABS/CS_0 = Chl/CS_0$	absorption flux per CS (at t = 0)
$TR_0/CS_0 = \varphi_{Po} \times (ABS/CS_0)$	trapped energy flux per CS (at t = 0)
$ET_0/CS_0 = \varphi_{Po} \times \psi_{Eo} \times (ABS/CS_0)$	electron transport flux per CS (at t = 0)
Density of RCs	
$RC/CS_0 = \varphi_{Po} \times (V_J/M_0) \times (ABS/CS_0)$	Q_A-reducing RCs per CS (at t = 0)
$S_m/t_{F_M} = [RC_{open}/(RC_{close} + RC_{open})]av = [Q_A/Q_{A(total)}]av$	average fraction of open RCs of PSII in the time span between 0 to t_{F_M}
Performance indexes	
$PI_{ABS} \equiv \frac{\gamma_{RC}}{1-\gamma_{RC}} \times \frac{\varphi_{Po}}{1-\varphi_{Po}} \times \frac{\psi_{Eo}}{1-\psi_{Eo}}$	performance index (potential) for energy conservation from photons absorbed by PSII to the reduction of intersystem electron acceptors
$PI_{total} \equiv PI_{ABS} \times \delta_{Ro}/(1 - \delta_{Ro})$	performance index (potential) for energy conservation from photons absorbed by PSII to the reduction of PSI end acceptors

© The authors. This is an open access article distributed under the terms of the Creative Commons BY-NC-ND Licence.